

P. Ayala, R. Arenal, M. Rummeli,  
A. Rubio and T. Pichler

*Review*  
The doping of carbon nanotubes with nitrogen and their potential applications

575

A. P. Merkle, A. Erdemir, O. L. Eryilmaz,  
J. A. Johnson and L. D. Marks

*Original Articles*  
*In situ* TEM studies of tribo-induced bonding modifications in near-frictionless carbon films  
Effect of functionalized carbon nanotubes on the thermal conductivity of epoxy composites

587

S.-Y. Yang, C.-C. M. Ma, C.-C. Teng,  
Y.-W. Huang, S.-H. Liao, Y.-L. Huang,  
H.-W. Tien, T.-M. Lee and K.-C. Chiu

Fabrication and characterization of magnetic cobalt ferrite/polyacrylonitrile and cobalt ferrite/carbon nanofibers by electrospinning

604

C.-T. Hsieh and W.-Y. Chen

Water/oil repellency and drop sliding behavior on carbon nanotubes/carbon paper composite surfaces

612

N. Larouche and B. L. Stansfield

Classifying nanostructured carbons using graphitic indices derived from Raman spectra

620

G. Srinivas, Y. Zhu, R. Piner, N. Skipper,  
M. Ellerby and R. Ruoff

Synthesis of graphene-like nanosheets and their hydrogen adsorption capacity

630

M. M. de Castro, M. Martínez-Escandell,  
M. Molina-Sabio and  
F. Rodríguez-Reinoso

Hydrogen adsorption on KOH activated carbons from mesophase pitch containing Si, B, Ti or Fe

636

G. Wei, C. Pan, J. Reichert and  
K. D. Jandt

Controlled assembly of protein-protected gold nanoparticles on noncovalent functionalized carbon nanotubes

645

C. Petit, K. Kante and T. J. Bandosz

The role of sulfur-containing groups in ammonia retention on activated carbons

654

S. Y. Sawant, R. S. Somani and  
H. C. Bajaj

A solvothermal-reduction method for the production of horn shaped multi-wall carbon nanotubes  
Nitrogen-containing graphitized carbon support for methanol oxidation Pt catalyst

668

D. B. Kim, D.-H. Lim, H.-J. Chun,  
H.-H. Kwon and H.-I. Lee

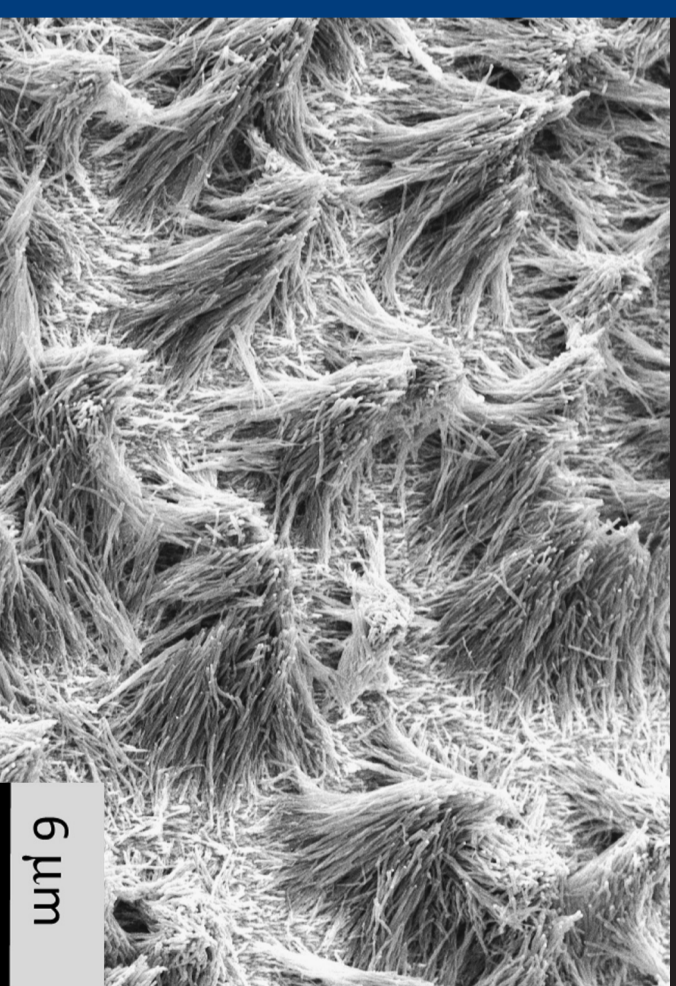
Investigation on sensitivity of a polymer/carbon nanotube composite strain sensor

680

(contents continued on inside back cover)



an international journal  
**Carbon**  
Reporting research on Carbonaceous Materials,  
their Production, Properties and Applications

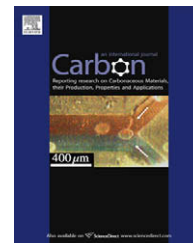


Editor-in-Chief: P.A. Thrower

Also available on ScienceDirect [www.sciencedirect.com](http://www.sciencedirect.com)



0008-6223(201003)48:3;1-#

available at [www.sciencedirect.com](http://www.sciencedirect.com)journal homepage: [www.elsevier.com/locate/carbon](http://www.elsevier.com/locate/carbon)

# Enhanced field emission stability and density produced by conical bundles of catalyst-free carbon nanotubes

Archana Pandey, Abhishek Prasad, Jason Moscatello, Benjamin Ulmen, Yoke Khin Yap \*

Department of Physics, Michigan Technological University, 118 Fisher Hall, 1400 Townsend Drive, Houghton, MI 49931, USA

## ARTICLE INFO

### Article history:

Received 8 July 2009

Accepted 8 September 2009

Available online 11 September 2009

## ABSTRACT

Self-assembled bundling and catalyst removal can enhance the field emission stability and density of vertically-aligned multiwalled carbon nanotubes (VA-MWCNTs). These catalyst-free, opened tip, VA-MWCNTs offered better emission stability than the as grown samples. Both the emission stability and density were further enhanced as the opened-tip MWCNTs self-assembled into arrays of conical bundles. Theoretical simulation suggests that higher emission density was due to the reduced screening effects. The simulated local fields at the tips of the bundles suggest for a two-order of magnitude lower electric field loading on MWCNTs and contribute to prolong emission stability needed for practical applications.

© 2009 Elsevier Ltd. All rights reserved.

## 1. Introduction

Carbon nanotubes (CNTs) are promising materials for electron field emission due to their small tip radius, high aspect ratio, and robust mechanical and chemical properties [1–4]. Although field emission from CNTs was known for more than a decade [5], reliable commercial products are yet to be realized. Obviously, the basic science for stable field emission with high emission density is still not clear. Most reported work focus on demonstrating low emission threshold fields ( $E_{th}$ ) of various types of CNTs [5–9] and their device configuration [10]. Recently, we started to investigate factors that determine the emission stability of CNTs and found that the graphitic order of CNTs is one of the key factors for stable emission [11]. In this paper, we found that both screening effects and catalyst removal are important for improving the emission stability and density of vertically-aligned multiwalled carbon nanotubes (VA-MWCNTs). Although screening effect was known to determine the emission density, its contribution to emission stability is not clear [8]. On the other hand, there is an ongoing controversy whether opening the tips of CNTs will enhance their field emission. In some cases, opened-tip CNTs contribute to lower emission threshold

fields ( $E_{th}$ ) [12]. However, other reported on emission degradation for opened-tip MWCNTs [13–15]. Here we report our experimental and theoretical finding related to these topics.

## 2. Experimental procedure

Our samples were prepared by dual RF-plasma-enhanced chemical vapor deposition [16]. In brief, Ni films (10 nm thick) were first deposited on *p*-type Si substrates (1–10  $\Omega$  cm) by RF magnetron sputtering. These substrates were then used for the growth of VA-MWCNTs at 450 °C by using pure methane gas. Our VA-MWCNTs were grown within a circular area (7 mm in diameter). Three identical samples can be prepared in each growth process. The residual Ni catalytic nanoparticles in our samples can be removed from the tips of VA-MWCNTs by etching in HNO<sub>3</sub> acid (70 vol.%, for ~5 min). The etched samples were then rinsed with de-ionized water and toluene. These processes lead to catalyst-free MWCNTs.

## 3. Results and discussion

All of our samples were characterized by field emission scanning electron microscopy (FESEM) and Raman spectroscopy

\* Corresponding author: Fax: +1 906 487 2933.

E-mail address: [ykyap@mtu.edu](mailto:ykyap@mtu.edu) (Y.K. Yap).

0008-6223/\$ - see front matter © 2009 Elsevier Ltd. All rights reserved.

doi:10.1016/j.carbon.2009.09.031

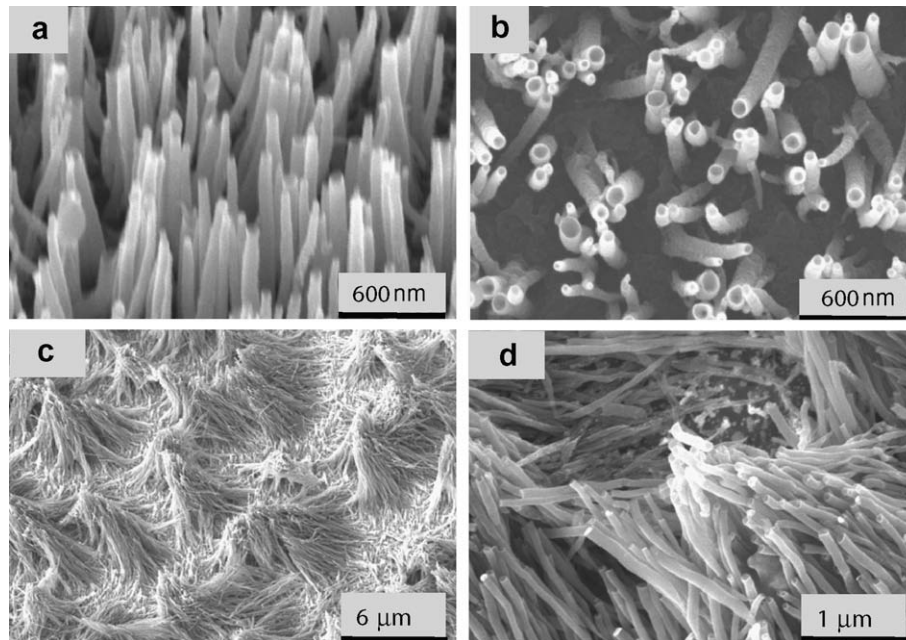


**Fig. 1** – Typical appearance of opened-tip VA-MWCNTs (a and b) and arrays of opened tip, conical bundles and low (c) and high (d) magnification.

(laser wavelength  $\sim 632$  nm, laser spot size  $\sim 1$   $\mu\text{m}$  in diameter). The field emission measurements were conducted in a planar diode configuration at a base vacuum pressure of  $10^{-7}$  mbar [17]. The spacing between the anode (Indium Tin Oxide/ITO film on glass) and the tips of the VA-MWCNTs was maintained at  $1000 \pm 10$   $\mu\text{m}$  without using dielectric spacer. All measurements were re-confirmed by repeating measurement on the same sample as well as another set of sample prepared in the same growth process and treatment.

As shown in Fig. 1a and b, we found that rinsing of toluene after acid etching can maintain the vertical alignment of the opened-tips MWCNTs. Tentatively we think that this is due to the lower surface tension of toluene than water ( $\sim 0.0287$

versus 0.0735). Lower surface tension will reduce the van der Waals forces between CNTs and toluene that will pull CNTs to each other during the drying process. However, toluene alone is insufficient to maintain the vertical alignment of VA-MWCNTs that are smaller in diameters. As shown in Fig. 1c and d, VA-MWCNTs with diameters  $< 60$  nm will self-assembled into conical bundles after etching. Obviously, the function of toluene (versus water) on maintaining the vertical alignment of these VA-MWCNTs would be an interesting topic for future investigation.

We have first compared as grown MWCNTs with the opened-tip, catalyst-free VA-MWCNTs. The appearance of the as grown sample (left inset) and their Raman spectra

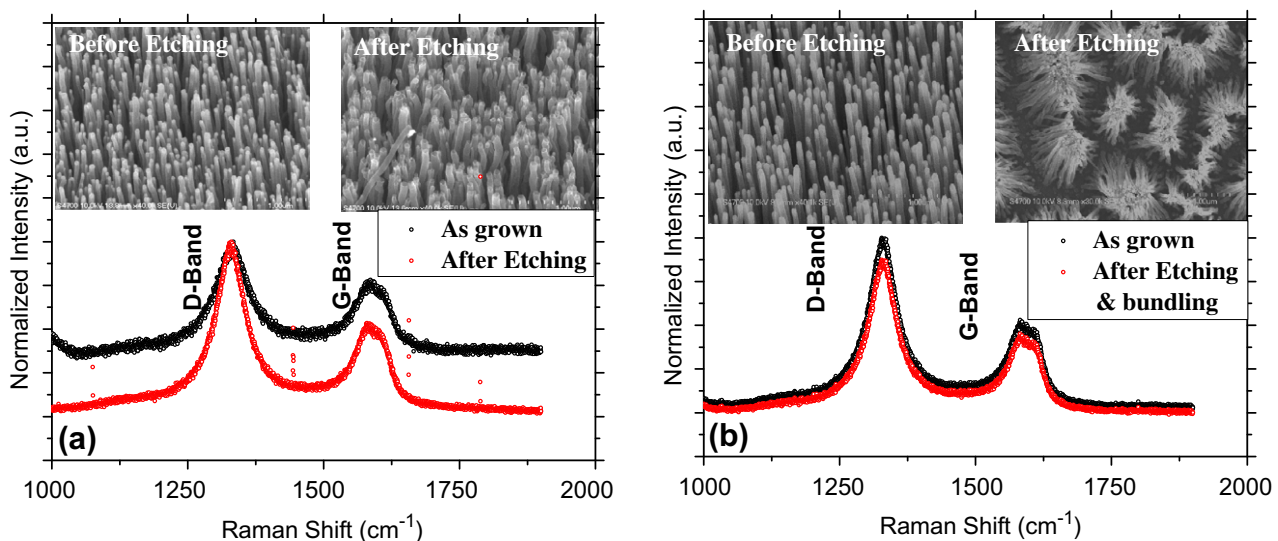


**Fig. 2** – (a) Raman spectra for the first set of samples. The as grown and the etched VA-MWCNTs are shown in the insets. (b) Raman spectra for the second set of samples. The as grow and the etched and bundled samples shown in the insets.

are shown in Fig. 2a. These VA-MWCNTs were  $\sim 4 \mu\text{m}$  in length and  $\sim 80 \text{ nm}$  in diameter. The graphitic order of these MWCNTs was examined by comparing the intensity of the graphitic (G) and defective (D) Raman bands. The G and D bands represent the zone center phonons of  $E_{2g}$  symmetry and the K-point phonons of  $A_{1g}$  symmetry, respectively [18]. The intensity ratio ( $I_G/I_D$ ) for the as grown and the etched VA-MWCNTs are  $\sim 0.88$  and  $\sim 0.78$ , respectively as shown in Fig. 2a. The difference is within the measurement deviation within a sample. For the second set of samples, the  $I_G/I_D$  ratios for the as grown and the etched and bundled samples remain at  $\sim 0.75$  as shown in Fig. 2b. From these results, we conclude that etching will not change the graphitic order of MWCNTs since carbon are inert to acids.

Fig. 3a shows the current density ( $J$ ) versus electric field ( $E$ ) characteristics for as grown VA-MWCNTs sample. The Fowler–Nordheim (FN) equation [19],  $J = A\beta^2 E^2 \exp(-B\phi^{3/2}/\beta E)$  is often use to describe field emission, where  $A, B$  are constants,  $E$  is the applied electric field in  $\text{V cm}^{-1}$ , and  $\phi$  is the work function in eV,  $\beta$  is the field enhancement factor. A linear FN plot (inset of Fig. 3a) verified that the detected currents are due to quantum tunneling. The threshold electric field,  $E_{\text{th}}$  (applied electric field for generating a current density of  $1 \mu\text{A/cm}^2$ ) is  $3.10 \text{ V}/\mu\text{m}$  for the as grown sample. The  $J$ – $E$  and

corresponding FN plots for the etched VA-MWCNTs are also shown in Fig. 3a. This etched sample has identical  $E_{\text{th}}$  and showing linear FN relation. The emission stability of these two samples was then compared. As shown in Fig. 3b, the etched VA-MWCNTs seem to have smaller degradation in current density after  $\sim 1200 \text{ min}$  of emission test. Apparently, the removal of residual catalyst particles from the tips of VA-MWCNTs does not reduce  $E_{\text{th}}$  but can improve the long-term emission stability. We think that residual metallic catalytic particles that have lower melting point than CNTs ( $\sim 1452 \text{ }^\circ\text{C}$  for bulk nickel versus  $>3650 \text{ }^\circ\text{C}$  for graphite) may create some unknown effects on the emission stability when significant Joule heating was introduced during the prolong emission stability test. The actual mechanism is not clear at present and is subjected for future investigation.

We have tested the second set of samples (tube diameter  $\sim 60 \text{ nm}$ ) to understand the effect of bundling. As shown in Fig. 3c,  $E_{\text{th}} \sim 2.60 \text{ V}/\mu\text{m}$  are detected from both the as grown and the etched and bundled samples. The linear FN relations (inset of Fig. 3c) were also revealed. Current saturation at high applied fields is detected in these samples. We think that electron supply is limited by the impedance (mostly resistance, but may include some capacitance and inductance) present especially along the CNTs and at the contacts

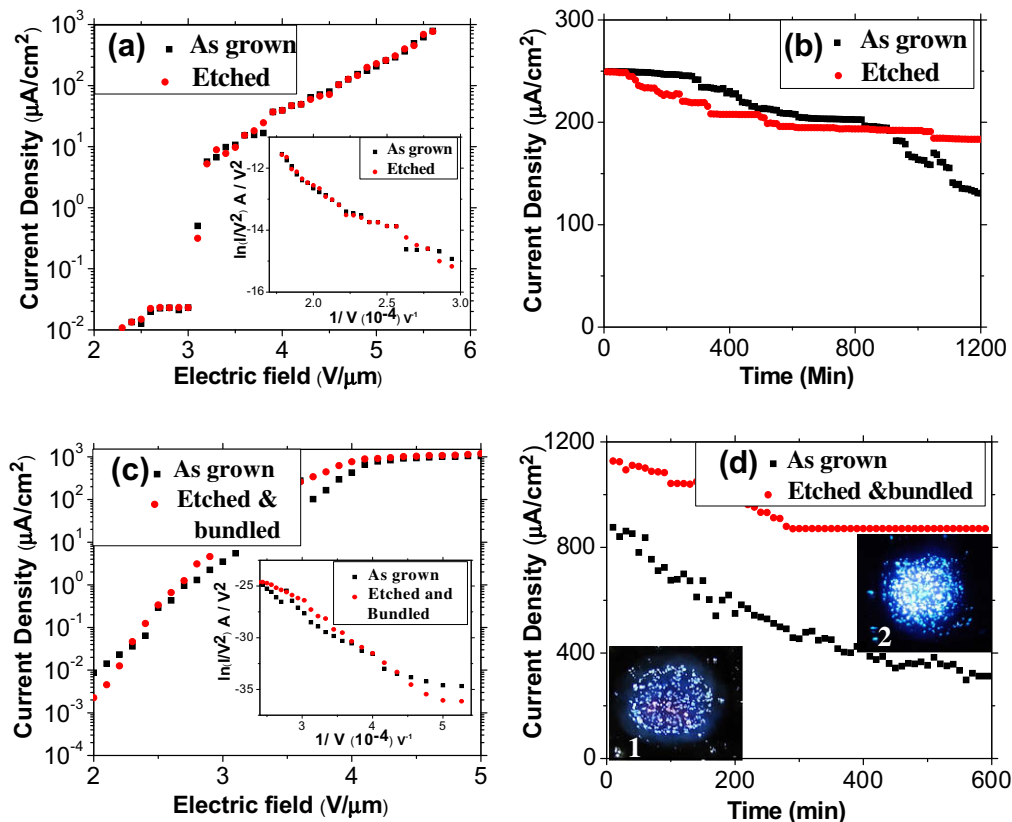
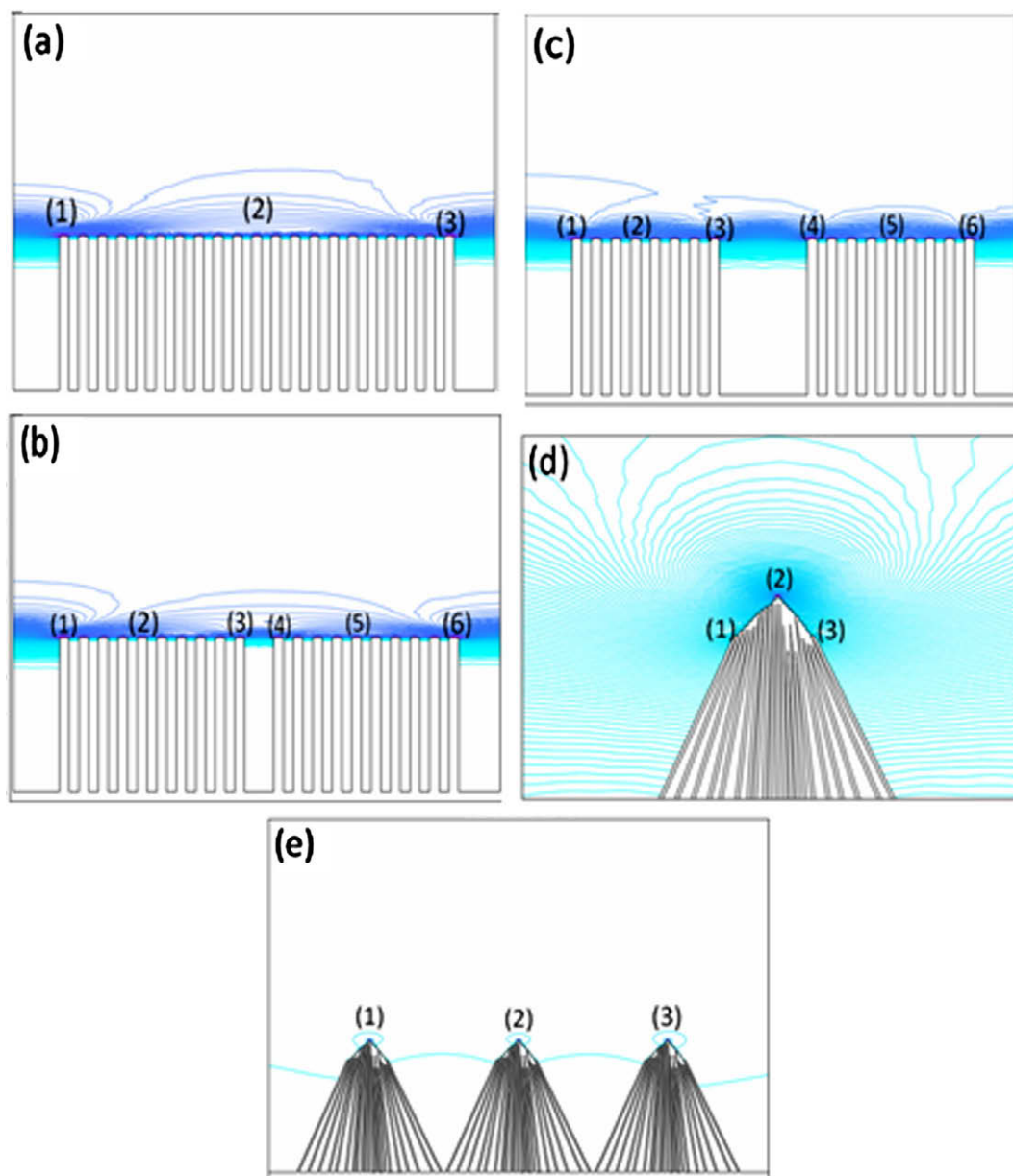


Fig. 3 – (a) The field emission characteristic curves for the as grown and the etched VA-MWCNTs shown in the insets of Fig. 2a. The related Fowler–Nordheim (FN) plots are shown in the insets. (b) The related emission current stability curves. (c) The field emission characteristic curves for the as grown and the etched and bundled MWCNTs shown in the insets of Fig. 2b. The related Fowler–Nordheim (FN) plots are shown in the insets. (d) The related emission current stability curves. Insets in (d) show the florescence on the ITO electrode as induced by the emitted electrons from the as grown (Inset 1) and the etched and bundled (Inset 2) CNTs.

between the CNTs and the substrate. These limiting factors become obvious at high current density probably due to Joule heating and/or current-induced dislocation [11]. As shown in Fig. 2a, the distances between the as grown VA-MWCNTs are small ( $\sim 50\text{--}300\text{ nm}$ ) and will initiate screening effect that reduced the  $\beta$  factors. This means not all the as grown VA-MWCNTs will contribute to the collected current except those are longer in lengths or located at the edges of the larger spacing. For the etched and bundled sample shown in Fig. 2b, the distances between bundles are more than one micrometer. Thus, each bundle can be considered as a larger emission pyramid. We have compared these samples for their emission stability. As shown in Fig. 3d, the etched and bundled sample is stabilized at a current density  $>800\ \mu\text{A}/\text{cm}^2$  after continu-

ous 20-h operation, while the as grown sample has reduced its current density to  $<400\ \mu\text{A}/\text{cm}^2$ . As shown in the insets of Fig. 3d, the emission density for the etched and bundled sample (inset 2) is higher than that of the as grown sample (inset 1). Apparently, lower screening effects on the bundled sample offers more emission sites. Since the emission loads (heat and mechanical stress from Joule heating) is now shared by more CNTs, the emission stability is thus improved. Theoretical simulation (to be discussed hereafter) suggests that lower local electric field is applied on these bundles. As indicated by the FN equation, a lower local field on each emitter will lead to the emission of lower current density per emitter. This will reduce Joule heating and stresses on these emitters and thus produce stable emission.



**Fig. 4** – Schematic of the simulated potential maps for (a) an array of VA-MWCNTs, (b) two arrays of VA-MWCNTs with a 120 nm spacing in between, (c) two arrays of VA-MWCNTs with a 280 nm spacing in between, (d) a conical bundle, and (e) three conical bundles.

It is interesting to see that both the as grown and bundled samples are by chance having identical  $E_{th}$ . This is explained as follows. The measured emission current from a sample is actually depends on both the current emitted from each emitters and the emitter density. Thus  $E_{th}$  is also depends on these factors. As our bundled sample has an  $E_{th}$  identical to that of the as grown sample, its higher emitter density suggests that the current emitted from each emitter in the bundled sample should be lower than that in the as grown sample. This interpretation is consistent to the results generated from our simulation to be described hereafter.

To further support our discussion, we have performed simulation by using the COMSOL™ MULTIPHYSICS software (Parameters: diameter of CNTs,  $D_{CNTs} = 40$  nm; Length of CNTs,  $L_{CNTs} = 4$   $\mu$ m; edge to edge spacing between CNTs,  $S = 40$  nm; applied electric field between top and bottom boundaries,  $E_{appl} = 5$  V/ $\mu$ m). Simulation for an array of VA-MWCNTs (Fig. 4a) shows that CNT at the center has lowest local electric field due to the screening effects from the surrounding CNTs ( $6.713 \times 10^6$  V/m at point 2 versus  $\sim 1.035 \times 10^7$  V/m and  $\sim 1.038 \times 10^7$  V/m at points 1 and 3, respectively). We further simulate the effect of the gap ( $S$ ) between two small arrays of VA-MWCNTs. Fig. 4b shows two arrays of VA-MWCNTs with  $S = 120$  nm. We observe that the local fields at both sides of the gap (point 3:  $\sim 9.15 \times 10^6$  V/m, and point 4:  $\sim 8.91 \times 10^6$  V/m) are higher than those at the centers of the two arrays (points 2:  $\sim 5.55 \times 10^6$  V/m, and point 5:  $\sim 5.48 \times 10^6$  V/m). Highest field is still observed at points 1 and 6 ( $\sim 1.037 \times 10^7$  V/m and  $\sim 1.027 \times 10^7$  V/m), i.e., edges close to the boundaries where no CNTs (and no screening effect) is found at one side. We have compared this to the case with  $S = 360$  nm. We observe that the local fields at points 3 and 4 ( $\sim 1.041 \times 10^7$  V/m and  $\sim 1.064 \times 10^7$  V/m) is higher than those at points 2 and 5 ( $\sim 6.30 \times 10^6$  V/m and  $\sim 7.65 \times 10^6$  V/m) and comparable to those at points 1 and 6 ( $\sim 1.022 \times 10^7$  V/m and  $\sim 1.068 \times 10^7$  V/m). We thus conclude that screening effect has reduced as the gap between CNT arrays increased to 360 nm.

We have simulated the local electric field for one conical bundle of CNTs as shown in Fig. 4d. The local field at point 2 ( $\sim 5.9743 \times 10^4$  V/m) is more than those at points 1 and 3 ( $\sim 4.058 \times 10^4$  V/m and  $\sim 3.712 \times 10^4$  V/m). This means, emission is more likely from CNTs located near the center of the bundles. Also, these values are two-order of magnitude lower than those discussed earlier for CNT arrays. As suggested by the FN equation, lower local fields on the bundles means lower current density will be emitted from each bundle, as consistent to our earlier interpretation. This means, heat and mechanical stresses introduced on CNTs due to Joule heating are lower for the case of nanotube bundles. Finally, we have simulated electric field applied on an array of CNT bundles. As shown in Fig. 4e, electric fields are  $\sim 6.2182 \times 10^4$  V/m,  $\sim 5.2582 \times 10^4$  V/m, and  $\sim 6.789 \times 10^4$  V/m at bundle 1, 2 and 3, respectively. Since the local field at bundle 2 is approaching that simulated in Fig. 4d (which has minimum screening effect), this means, the investigated gap ( $S = 2$   $\mu$ m) between bundles is sufficient to reduce the screening effects and enabled emission from most bundles. This is consistent to the higher emission density shown in Fig. 3d. As the collected current is contributed by more emission sites, the current loading

on individual bundles is lower as compared to the loading on individual CNTs in the case of CNT arrays.

#### 4. Summary

In summary, we found that opened-tip VA-MWCNTs can produce more stable emission. Bundling of these VA-MWCNTs can further reduce the screening effects, increase the emission density, and improve the emission stability. These results are confirmed by theoretical simulation, which further suggests that a two-order of magnitude lower electric field loading are applied on these bundles that reduce current loading, thermal and mechanical stresses and thus enhance the emission stability.

#### Acknowledgements

This work was supported by the Defense Advanced Research Projects Agency (Contract number DAAD17-03-C-0115 through the US Army Research Laboratory), and the US Department of Army (Grant number W911NF-04-1-0029 through the City College of New York). Contributions from Lakshman Kumar Vanga, Jitendra Menda, Adam DeConinck, Vijaya Kayastha, and Jiesheng Wang, are acknowledged.

#### REFERENCES

- [1] Ijima S. Helical microtubules of graphitic carbon. *Nature* (London) 1991;354:56–8.
- [2] Treacy MMJ, Ebbesen TW, Gibson JM. Exceptionally high Young's modulus observed for individual carbon nanotubes. *Nature* (London) 1996;381:678–80.
- [3] Dresselhaus MS, Dresselhaus G, Avouris P. Carbon nanotubes: synthesis, structure, properties, and application. Berlin: Springer; 2001. p. 287–320.
- [4] Walters DA, Ericson LM, Casavant MJ, Liu J, Colbert DT, Smith KA, et al. Elastic strain of freely suspended single-wall carbon nanotube ropes. *Appl Phys Lett* 1999;74:3803–5.
- [5] deHeer WA, Chatelain A, Ugarte D. A carbon nanotube field-emission electron source. *Science* 1995;270:1179–80.
- [6] Collins PG, Zettl A. A simple and robust electron beam source from carbon nanotubes. *Appl Phys Lett* 1996;69:1969–71.
- [7] Choi WB, Chung DS, Kang JH, Kim HY, Jin YW, Han IT, et al. Fully sealed, high-brightness carbon-nanotube field-emission display. *Appl Phys Lett* 1999;75:3129–31.
- [8] Nilsson L, Groening O, Emmenegger C, Kuettel O, Schaller E, Schlapbach L, et al. Scanning field emission from patterned carbon nanotube films. *Appl Phys Lett* 2000;76:2071–3.
- [9] Bonard JM, Klinke C, Dean KA, Coll BF. Degradation and failure of carbon nanotube field emitters. *Phys Rev B* 2003;67:115406–10.
- [10] Han IT, Kim HJ, Park Y, Lee N, Jang JE, Kim JW, et al. Fabrication and characterization of gated field emitter arrays with self aligned carbon nanotubes grown by chemical vapor deposition. *Appl Phys Lett* 2002;81:2070–2.
- [11] Kayastha VK, Ulmen B, Yap YK. Effect of graphitic order on field emission stability of carbon nanotubes. *Nanotechnology* 2007;18:035206-1–4.
- [12] Rinzler AG, Hafner JH, Nikolaev P, Nordlander P, Colbert DT, Smalley RE, et al. Unraveling nanotubes: field emission from an atomic wire. *Science* 1995;269:1550–3.

- [13] Saito Y, Hamaguchi K, Uemura S, Uchida K, Tasaka Y, Ikazaki F, et al. Field emission from multi-walled carbon nanotubes and its application to electron tubes. *Appl Phys A* 1998;67:95–100.
- [14] Bonard JM, Salvétat JP, Stockli T, Forro L, Chatelain A. Field emission from carbon nanotubes: perspectives for applications and clues to the emission mechanism. *Appl Phys A* 1999;69:245–54.
- [15] Bonard JM, Kind H, Stockli T, Nilsson LO. Field emission from carbon nanotubes: the first five years. *Solid-State Electron* 2001;45:893–914.
- [16] Menda J, Ulmen B, Vanga LK, Kayastha VK, Yap YK, Pan Z, et al. Structural control of vertically aligned multiwalled carbon nanotubes by radio-frequency plasmas. *Appl Phys Lett* 2005;87:173106-1–3.
- [17] Ulmen B, Kayastha VK, DeConinck A, Wang J, Yap YK. Stability of field emission current from various types of carbon nanotube films. *Diamond Relat Mater* 2006;15:212–6.
- [18] Yap YK, Kida S, Aoyama T, Mori Y, Sasaki T. Influence of negative dc bias voltage on structural transformation of carbon nitride at 600 °C. *Appl Phys Lett* 1998;73:915–7.
- [19] Fowler RH, Nordheim L. Electron emission in intense electric fields. *Proc R Soc A* 1928;119:173–81.